# *Rock Mass – Tunnel Support Interaction Analysis: Part II – Support Reaction Curves*


***M.N. Viladkar*[1]**
***M. Verman*[2]**
***Bhawani Singh*[3]**
***and***
***J.L. Jethwa*[4]**

[1]*Department of Civil Engineering*
*Indian Institute of Technology Roorkee*
*Roorkee – 247667, India*
*E-mail: sumanfce@iitr.ernet.in*

[2]*Advanced Technology Engineering Services*
*New Delhi, India*

[3]*(Retd.), Department of Civil Engineering*
*Indian Institute of Technology Roorkee*
*Roorkee – 247667, India*

[4]*(Retd.), Central Institute of Mining and Fuel Research*
*Regional Centre, Nagpur, India*

## ABSTRACT

The rock mass – tunnel support interaction analysis consists mainly of two stages. Prediction of ground response characteristics forms the first component which has been discussed in Part-I of this paper. This paper, which forms Part - II, deals primarily with an approach for realistic determination of support reaction curves and the support pressures. The approach has been proposed on basis of the field studies discussed in Part-I of the paper. Using this data, correlations have also been presented here for estimation of the stiffness of backfill material between support system and the rock mass, post construction saturation pressures and the stand-up time for flat and arch tunnel roofs.

***Keywords:*** Rock mass; Tunnel support interaction; Support reaction curve.

## 1. INTRODUCTION

The analysis of tunnel support behavior has received relatively less attention. Various authors (e.g. Lombardi, 1970; Daemen, 1975; Hoek and Brown, 1980) presented similar expressions for stiffnesses for different types of support systems considering linear elastic behavior. Stille et al. (1989) and Indraratna and Kaiser (1990) presented elasto-plastic analysis of rock mass supported with grouted rock bolts and Mitri and Hassan

(1990) have discussed the behavior of steel supports in coal mines using non-linear finite element analysis. A large number of research workers have reported the use of field instrumentation in tunnels driven in varying ground conditions. Significant conclusions have been drawn on the basis of these field studies regarding the ground and the support behavior, support requirements, method of support design, method and sequence of excavation and the benefits of NATM.

## 2. STATEMENT OF PROBLEM

A critical study of the literature highlights the fact that determination of the support reaction curve has not yet received adequate attention. The support behavior has been, by and large, assumed to be linear elastic which is not realistic due to the non-linear behavior of the support backfill. The variation of backfill stiffness with support pressure has also not been investigated. The influence of parameters like, the distance to the face of advance, tunnel size and post construction saturation of rock mass due to charging of the water conductor system, on support pressure has not been studied from the point of view of the rock mass-tunnel support interaction. Finally, rigorous analytical solutions proposed by various research workers are not very easy for the field engineers to implement at the site for quick estimation and revision, if required, of the support requirements during construction. In view of this, Verman (1993) developed simple, yet reliable, approach for determination of the support reaction curve directly from the data of instrumented tunnels.

## 3. DETERMINATION OF SUPPORT REACTION CURVE

Once the ground response curve has been obtained, the next step in rock mass – tunnel support interaction analysis is to determine the support reaction curve which establishes the relationship between tunnel deformation and the support pressure available from the support system. Based on the analysis of data collected from several tunnels in India (Tables 1 and 2, Viladkar et al., (2008)), the behavior of steel rib-backfill support system has been studied and an approach has been proposed here for determination of the support reaction curve.

The supports are usually installed after a certain amount of tunnel closure has occurred. This initial tunnel closure is denoted by $u_{ao}$ in Fig. 1a which shows an ideal support reaction curve characterized by a stiffness constant k. From Fig. 1a, the radial tunnel deformation, $u_a$ is given by:

$$u_a = u_{ao} + p_i \, a / k \qquad (1)$$

where $p_i$ is the short term support pressure; a is the tunnel radius and k is the stiffness of support system. Equation 1 remains valid till the maximum support system capacity is reached. Therefore, for obtaining the support reaction curve, the support stiffness as well as the maximum support capacity are required to be determined.

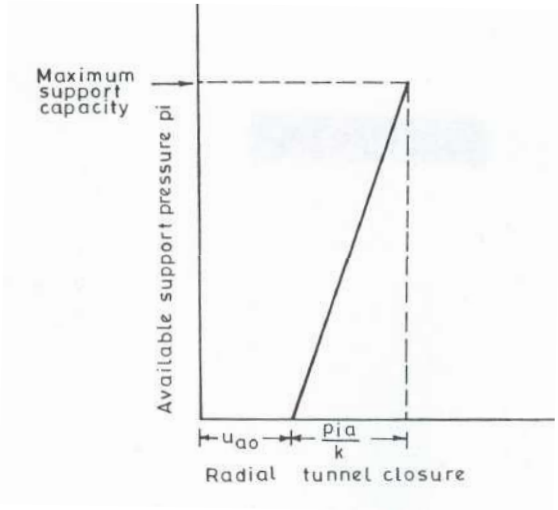


Fig. 1a - Linear support reaction curve with constant support stiffness

### 3.1 Stiffness of Steel Rib-Backfill Support System

At a tunnel section supported by steel ribs, backfill is placed between steel ribs and rock mass and is meant to provide an effective contact between them. Backfill itself is not designed to carry any load and its role is restricted to act as a packing (cushion) between the rock mass and steel ribs and facilitates the load transfer. Stiffness of the backfill plays an important role in determining the stiffness of the overall support system. A support system, comprising of steel ribs and backfill, can be assumed to be acting as two stiff springs connected in series. Therefore, overall stiffness of the support system is given by-

$$1/k = 1/k_s + 1/k_b \quad (2)$$

where k represents the overall stiffness of steel rib – backfill support system, $k_s$ is the stiffness of steel ribs and $k_b$ is the stiffness of backfill.

### 3.2 Stiffness of Steel Rib

Stiffness of steel ribs may be obtained from the following expression from the stiffness of a steel ring under an evenly distributed (external) pressure (Hoek and Brown, 1980):

$$k_s = E_s \cdot A_s / s \cdot a \quad (3)$$

where $E_s$ = the modulus of elasticity of steel; $A_s$ = the cross-sectional area of steel rib; s = the rib spacing and a = the tunnel radius.

### 3.3 Stiffness of Backfill

Field instrumentation data comprising of support pressures and tunnel deformations, obtained on basis of monitoring of several Indian Tunnels (Tables 1 and 2, Viladkar et al., 2008 Part-I in this issue of Journal ) were analyzed and the support reaction curves

were plotted for each instrumented tunnel section following the procedure outlined in Part-I of the paper in this issue of the Journal (Viladkar et al., 2008). This procedure gives the value of radial tunnel closure, $u_{ao}$ before installation of supports and the instrumentation. Figure 1b shows a typical observed support reaction curve plotted for a tunnel section at a chainage of 738.5 m in Maneri-Uttarkashi tunnel.

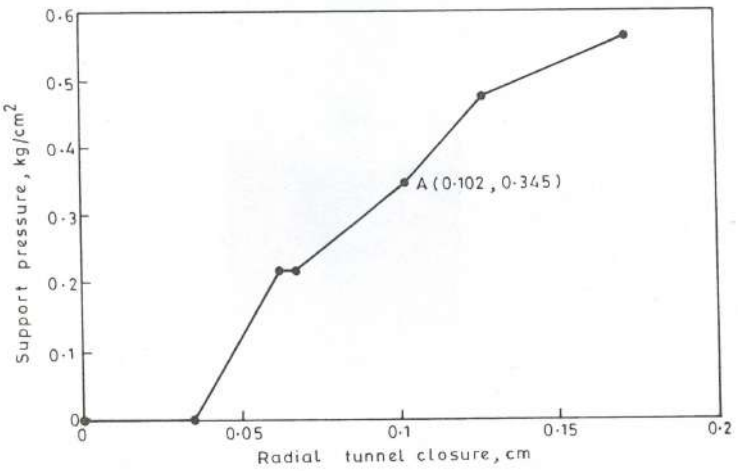


Fig. 1b - Observed support reaction curve for Ch. 738.5 m (D/S Maneri) in Maneri – Uttarkashi tunnel

The observed support reaction curve could then be back-analyzed. Knowing $u_{ao}$, and corresponding observed values of tunnel closure, $u_a$ and support pressure, $p_i$, the overall observed support stiffness, k was obtained from Eq. 1. Knowing this value of k and the support stiffness, $k_s$ of steel rib (Eq. 3), actual stiffness of backfill, $k_b$ could be obtained from Eq. 2. From the values of the backfill stiffness thus obtained for different tunnel sections, the following empirical correlation was obtained:

$$k_b = 1.16 \cdot t_b \cdot E_b / a^{1.05} \quad , \text{kg/cm}^2 \qquad (4)$$

where $t_b$ refers to the thickness of backfill in m, $E_b$ is the modulus of deformation of backfill in kg/cm$^2$ and a is the radius of tunnel opening in m.

One may take, for instance, point A in Fig. 1b for which $u_a$ = 0.102 cm and $p_i$ = 0.345 kg/cm$^2$. The value of $u_{ao}$ is 0.035 cm and the tunnel radius, a, at this section is 2.90 m. Substituting these values in Eq. 1,

$$0.102 = 0.035 + [(0.345)\ (290)/k]$$

from which, k = 1493 kg/cm$^2$. At this section, steel ribs having $E_s = 2.1 \times 10^6$ kg/cm$^2$, $A_s$ = 38.98 cm$^2$ and s = 80 cm, have been used. Equation 3, therefore, gives value of steel rib stiffness, $k_s$.

$$k_s = [(2.1 \times 10^6)\ (38.98)]/(80 \times 290) = 3528 \text{ kg/cm}^2$$

Substituting the values of k and $k_s$, thus obtained, in Eq. 2.

$$(1/1493) = (1/3528) + (1/k_b)$$

from which, $k_b = 2589$ kg/cm$^2$ which is the actual stiffness of backfill at point A on observed support reaction curve (Fig. 1b). Similarly, the value of $k_b$ can be obtained all along the observed support reaction curve for different observed values of $p_i$. This exercise was carried out for all instrumented tunnel sections to evaluate the variation of modulus of deformation of the backfill (which is related to backfill stiffness) with support pressure.

### 3.4 Variation of Modulus of Deformation of Backfill with Support Pressure

The support reaction curves for all the instrumented tunnel sections were observed to be non-linear, unlike the conventional theoretical assumption of a linear support reaction curve. The reason for this could be attributed to the change in the modulus of deformation of backfill, $E_b$, and, consequently in the backfill stiffness, $k_b$ with increasing support pressure, $p_i$. Whereas concrete was used as backfill at most of the instrumented sections, a few sections had gravel or tunnel-muck as backfill. This provided an opportunity to study the behavior of different types of backfills under pressure. Figures 2 a, b, c show the relationships between the modulus of deformation of different backfills and the support pressure, from which following correlations have been obtained:

i) for concrete backfill,

$$E_b = 137\, p_i^{0.77} \text{ to } 926\, p_i^{0.88} \quad \text{MPa} \qquad (5a)$$

ii) for gravel backfill,

$$E_b = 10\,(p_i + 65.16) \text{ to } 10\,(p_i + 14.65) \quad \text{MPa} \qquad (5b)$$

iii) for tunnel-muck backfill,

$$E_b = 54\, p_i^{0.215} \text{ to } 97\, p_i^{0.33} \quad \text{MPa} \qquad (5c)$$

In Eqs. 5a, 5b and 5c, $p_i$ is in kg/cm$^2$. For developing these correlations, modulus of deformation of the backfill, $E_b$ was back-calculated from the observed backfill stiffness, $K_b$ for different values of support pressure, $p_i$, using the following expression for the stiffness of a thick wall cylinder:

$$k_b = \frac{E_b[a^2 - (a - t_b)^2]}{(1+\nu_b)[(1-2\nu_b)a^2 + (a - t_b)^2} \qquad (6)$$

where $\nu_b$ is the Poisson's ratio of the backfill. Equation 6 is based on the assumption of a closed ring of backfill having uniform thickness, $t_b$ and much of the backfill stiffness derives from the continuity of this ring.

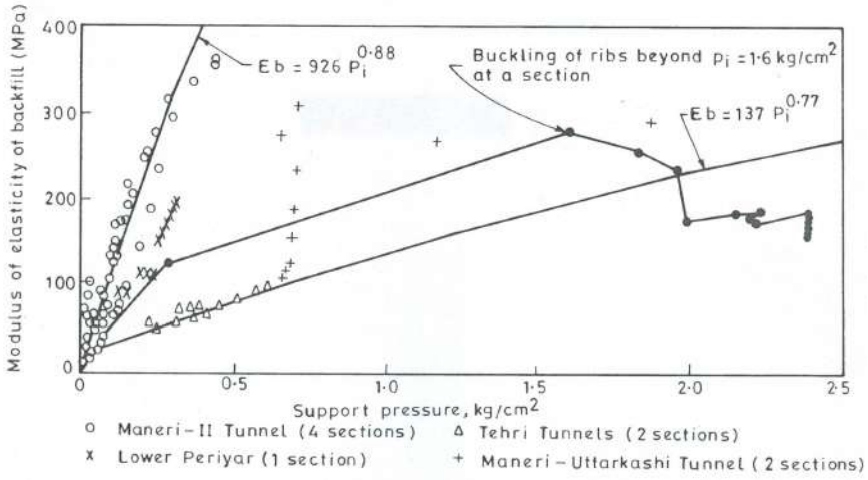


Fig. 2a - Variation of modulus of elasticity of concrete backfill with support pressure

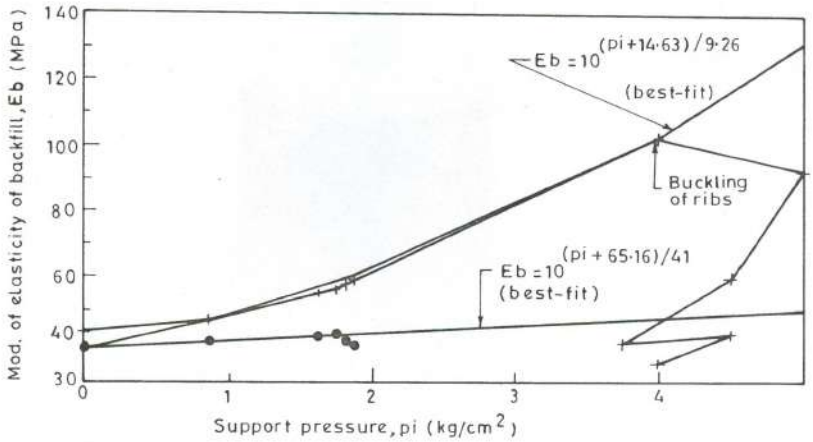


Fig. 2b - Variation of modulus of elasticity of gravel backfill with support pressure at two locations in Giri tunnel

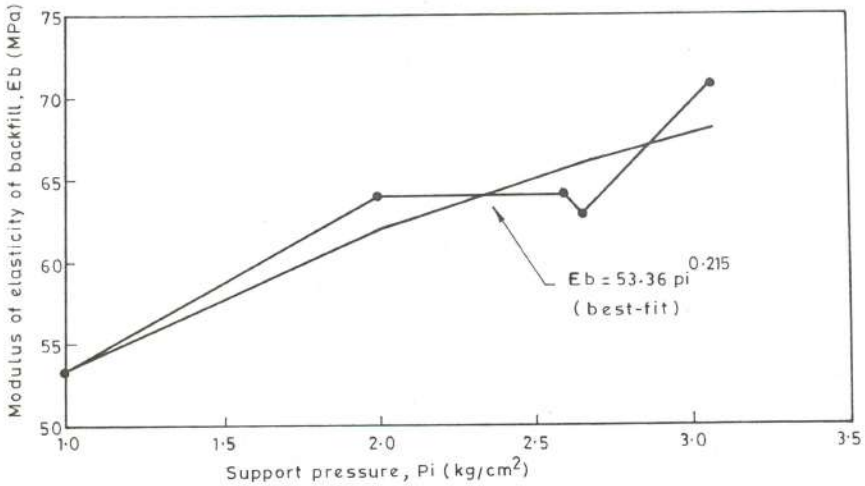


Fig. 2c - Variation of modulus of elasticity of tunnel muck with support pressure

### 3.5 Maximum Capacity of Steel Rib – Backfill Support System

The maximum support capacity of steel rib–backfill support system is governed by the maximum support capacity of the steel ribs, which is given by:

$$P_{i\,max} = \sigma_{ys} \,.\, A_s / (s \,.\, a) \qquad (7a)$$

where $P_{i\,max}$ is the maximum support capacity of steel ribs and $\sigma_{ys}$, yield strength of steel.

If the yield strength of steel is more than the buckling stress of steel rib, $\sigma_{ys}$ should be replaced by the buckling stress in Eq. 7a. The maximum support capacity will then be given by the equation (Timoshenko and Gere, 1961):

$$P_{i\,max} = 3 \,.\, E_s \,.\, I_s / (a^3 \,.\, s) \qquad (7b)$$

where, $I_s$ is the moment of inertia of the steel rib.

### 3.6 Support Reaction Curve

(i) The modulus of deformation, $E_b$ of the backfill can be estimated using either of Eqs. 5a, 5b and 5c.

(ii) Stiffness of backfill, $K_b$ can be estimated using this value of $E_b$ in Eq. 4.

(iii) The stiffness of steel ribs can be obtained from Eq. 3 and the overall stiffness, K of the combined support system can be obtained from Eq. 2.

(iv) Equation 1 can then be used to obtain different values of radial tunnel closure, $u_a$ for various values assigned to support pressure, $p_i$, and a plot of $p_i$ versus $u_a$ can be made. This plot may be superimposed on the ground response curve (Viladkar et al., 2008).

(v) The maximum support capacity of steel rib-backfill support system will be governed by either Eqs. 7a or 7b.

The support reaction curve, thus obtained, will be non-linear which is indicated by Eqs. 5 a, b, c derived on basis of actual field observations. Earlier authors (Lombardi, 1970, 1973; Ladanyi, 1974; Daemen, 1975; Hoek and Brown, 1980) did not consider the support pressure dependent modulus of deformation of the backfill and as such assumed the support reaction curves to be linear elastic.

### 3.7 Behavior of Different Types of Backfills

While studying the variation of modulus of deformation of different types of backfills with support pressure (Eqs. 5a, 5b and 5c), some interesting observations were made regarding the backfill behavior under pressure. These are as follows:

### *3.7.1 Concrete backfill*

Most of the instrumented tunnel sections were provided with concrete as the backfill. An example of typical behavior of concrete backfill, observed at majority of such sections, is shown in Fig. 3a which is a plot between the modulus of deformation of backfill and support pressure at a chainage of 829m in the head race tunnel-3 of Tehri Hydro Project (Table 1, Viladkar et al., 2008). It may be inferred that early stage concrete backfill cracks under low pressure soon after it is placed behind the ribs and looses its initial stiffness. This reduction in its stiffness continues until a stage is reached where cracked backfill is compacted due to increasing support pressure. Consequently, there is an again increase in its stiffness. Sometimes, initial reduction in stiffness is rapid as illustrated in Fig. 3b which pertains to Chainage 1568.5m in Maneri-Bhali Stage-II tunnel (Table 2, Viladkar et al., 2008). The overall trend was, however, observed to be similar at almost all the sections. At one of the sections (Chainage of 777m, u/s of Dhanarigad adit – Fig. 2a) in Maneri Bhali Stage-II tunnel, the steel ribs buckled under high squeezing pressure resulting in a sudden loss of contact between backfill and rock mass. This is indicated by a sudden drop in backfill stiffness after buckling of the ribs. An outcome of this study is that concrete, when used as backfill, is crushed almost immediately and looses whatever strength it had gained during a very short time interval between its mixing and placing behind the ribs. Therefore, it merely acts as a packing material which gains its stiffness from compaction of crushed particles. It would therefore be more appropriate to call it as 'packing concrete' or 'blocking concrete' instead of just 'concrete'.

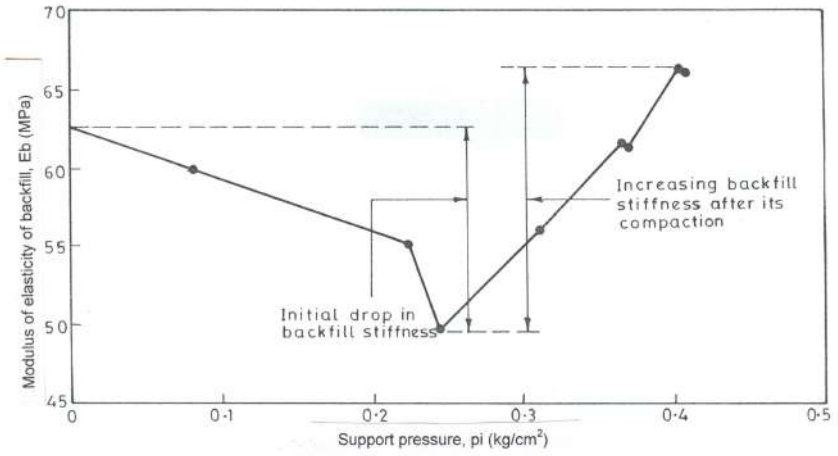


Fig. 3a - Initial drop in concrete backfill stiffness at Ch. 829 m in HRT – 3, Tehri project

### *3.7.2 Gravel backfill*

The gravel backfill does not show any initial loss of stiffness under pressure, as illustrated through an example of Giri tunnel in Fig. 2b. The stiffness increases with support pressure on account of increasing compaction of backfill which in the process gradually becomes more dense. This process continues till an equilibrium support pressure (as shown in Fig. 2b pertaining to a highly squeezing section) corresponding to

the maximum capacity of steel ribs is reached. Initially, the opening stabilizes and then steel supports buckle. The buckling of steel ribs under high pressure results in a sudden loss of contact between backfill and the rock mass. Consequently, the backfill stiffness drops sharply.

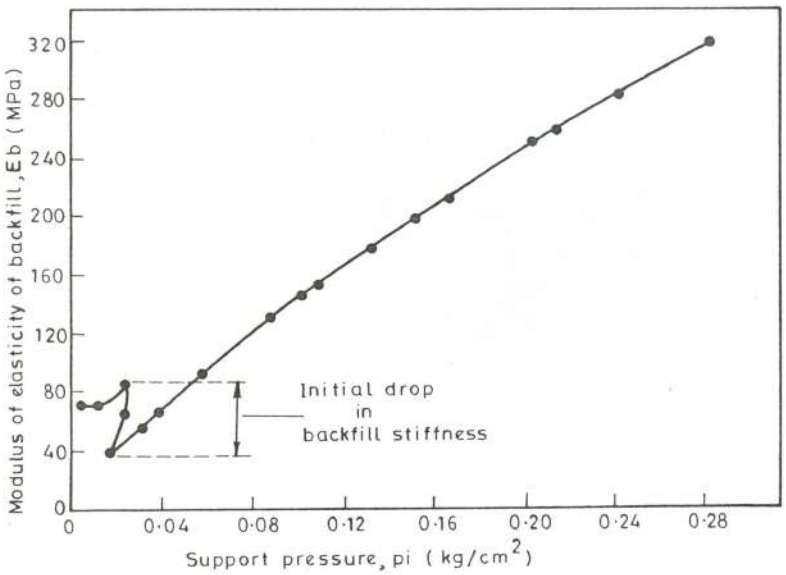


Fig. 3b - Rapid initial drop in concrete backfill stiffness at Ch. 1568.5m in Maneri Stage – II tunnel

*3.7.3 Tunnel-muck backfill*

The tunnel-muck backfill has an initial stiffness similar to the gravel backfill. It also shows an increasing trend with increase in support pressure (Fig. 2c; Chhibro-Khodri tunnel, Table 2 Chainage of 2575 m, Viladkar et al. 2008). However, the build-up of backfill stiffness with increase in support pressure is slower than that for the gravel backfill.

*3.7.4 Comparative behavior of backfills and suitability to different ground conditions*

The concrete backfill, despite an initial loss of stiffness, provides a stiffer support as compared to the gravel and the tunnel-muck backfills. It may be seen from Es. 5 a,b,c that for at a support pressure of 1 kg/cm$^2$, the modulus of deformation of concrete, gravel and tunnel-muck backfills ranges from 137 to 926, 54 to 97, and 41 to 49 MPa respectively. Concrete backfill is, therefore, preferable for non-squeezing ground condition. The tunnel-muck backfill may be more suited to moderately squeezing ground condition and the gravel backfill to highly squeezing ground condition, as the latter is more flexible. These two types of backfills are flexible initially and gradually become stiffer with increasing support pressure, thus accommodating large deformations which occur in squeezing ground conditions and thus permitting low support pressures.

## 4. ROCK MASS – TUNNEL SUPPORT INTERACTION ANALYSIS

Based on the data obtained from instrumentation and monitoring of tunnels in India, approaches have been proposed for prediction of ground response curve (Viladkar et al., 2008) and the support reaction curve, the two essential components of rock mass-tunnel support interaction analysis. The ground reaction curves may be obtained for squeezing and non-squeezing ground conditions (including the self-supporting condition) using an approach suggested in Part-I of this paper (Viladkar et al., 2008). This, together with the approach proposed here to obtain the support reaction curve, may be used to perform rock mass-tunnel support interaction analysis. An alternative to this approach has been suggested on basis of empirical ground response curve by Singh et al. (1992). Coordinates of the intersection point of these two curves define the support pressure and the radial deformation at which the rock mass-tunnel support system achieves equilibrium. Stability of the system depends upon whether the deformation experienced by the system is within the permissible limit or not. Supports installed too early will have to experience higher pressures but will undergo smaller deformations whereas supports with identical stiffness but installed too late will undergo large deformations and shall experience relatively much less support pressure, if delay is not beyond the stand up time of the rock mass.

Economy of the tunnelling project is directly affected by the stiffness of the support system. Too stiff support system will mean lesser deformations and therefore a stable system but will invite higher support pressures and the consequent loss of economy whereas, a very flexible support system will experience less pressures and will be economical but will experience large deformations endangering the stability of tunnel (Fig. 1 in Part I; Viladkar et al., 2008). In real field situations, however, some kind of balance has to be struck between *too early and too late* installation of supports and *too stiff and too flexible* support systems. Ideally, delay in support installation should not be beyond the stand up time.

## 5. EFFECT OF CHARGING OF WATER CONDUCTOR SYSTEM ON SUPPORT PRESSURE

When a hydro power project is commissioned, rock mass surrounding the underground excavations gets saturated due to the water conductor system. As a result, additional pressure builds up on rigid concrete lining. It is, therefore important to consider this additional effective support pressure while designing the lining. Rock mass-tunnel support interaction analysis can also help in determining this additional support pressure.

Figure 4 shows schematically the ground response curves for both dry and saturated conditions in non-squeezing ground along with the support reaction curve. Upon charging of the system, modulus of deformation of rock mass reduces due to saturation and ground response curve shifts from the path AB to AC, putting an additional pressure, BC on the concrete lining. Using Eq. 5 presented in Part I of this paper (Viladkar et al., 2008) for both dry and saturated conditions of rock mass, following expression has been obtained for this additional effective support pressure $\Delta p_{isat}$ :

$$\Delta p_{isat} = [1 - ( E_{sat} / E_{dry} ) ( p_o - p_{i\,dry} )] \quad (8)$$

where $E_{sat}$ represents the modulus of deformation of saturated rock mass, $E_{dry}$ is modulus of deformation of dry rock mass, and $p_{i\,dry}$ is the short-term support pressure in dry condition. Derivation of Eq. 8 is presented in Appendix-A.

It may be noted that rock mass is assumed to be saturated everywhere after charging of the water conductor system. This assumption would be valid only if the internal water pressure head ( $p_w / \gamma_w$ ) is more than, say, three times the diameter of the tunnel. This is generally the case in hydro-electric projects. According to Mehrotra (1992),

$$(E_{sat} / E_{dry}) = 0.016\ RMR - 0.385 \quad \text{(for RMR = 41 to 60)} \quad (9a)$$

$$= 0.010\ RMR - 0.10 \quad \text{(for RMR < 41 an rock with water sensitive minerals)} \quad (9b)$$

Substitution of above values of ( $E_{sat} / E_{dry}$ ) in Eq. 8 for RMR > 30 in non-squeezing ground condition, results in the following expressions:

$$\Delta p_{i\,sat} / p_o = 0 \text{ to } 0.8 [1 - ( p_{i\,dry} / p_o )] \quad (10)$$

Equation 10 may be used to estimate the additional support pressure due to charging of water conductor system in non-squeezing ground condition. It may be seen that for lower values of the ratio, $p_{i\,dry} / p_o$ build-up of additional support pressure is high. Since in practice, values of $p_{i\,dry} / p_o$ are very low, $\Delta p_{i\,sat} / p_o$ lies in a range of very high values and the additional support pressure may be as high as about 80 percent of the in-situ stress. The proposed simple analysis is intended to justify the urgent need for simulating the effect of post-construction saturation in the computer modelling of rock structures.

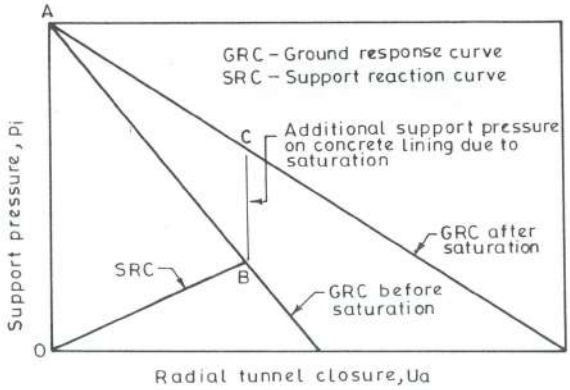


Fig. 4 - Effect of rock mass saturation on support pressure

## 6. EXPRESSION FOR SUPORT PRESSURE IN NON-SQUEEZING GROUND CONDITION AND EFFECT OF TUNNEL SIZE

Short-term support pressure or support pressure at equilibrium, i.e., when ground response and the support reaction curves intersect, can be expressed as-

$$p_{if} = \frac{[(1+\nu)p_o / E_d - (u_{ao}/a)]}{(1+\nu)/E_d + (s..a/E_s.A_s) + (0.86a^{1.05}/t_b.E_{bf})} \quad (11a)$$

where $p_{if}$ is the Short-term support pressure (i.e. support pressure at equilibrium) and $E_{bf}$ is the modulus of deformation of backfill at support pressure equal to $p_{if}$. Derivation of Eq. 11a is presented in Appendix-B.

It may be seen from Eq. 11a that short-term support pressure would be practically independent of the tunnel size, a if values of $A_s$ /s and $t_b$ are increased in direct proportion to the tunnel size. Equation 11a may be generalized to include the effect of anisotropy of rock mass, additional support pressure ($p_{i\ sat}$ from Eq. 8) due to charging of the water conductor system and the seepage pressure. The generalized equation is the sum of all the three types of support pressures as given below:

$$p_{if} = \frac{[(1+\nu)p_o / RF.E_{min} - (u_{ao}/a)]}{[(1+\nu)/RF.E_{min} + (s.a/E_s.A_s) + (0.86a^{1.05}/t_b.E_{bf})]} + p_{isat} \quad (11b)$$

where, RF is the reduction factor, which together with $E_{min}$ accounts for the anisotropy of rock mass, $E_{min}$ is the smaller of the two moduli of deformation of rock mass in horizontal and vertical directions and $p_w$ is the seepage pressure on the tunnel lining. The value of reduction factor, RF has been derived by analyzing the numerical model of a lined tunnel (Kumar and Singh, 1990). The whole approach is based on the continuum characterization of anisotropic rock mass (Singh, 1973) in which the elastic properties of rock mass are reduced depending upon the discontinuity description and their spacings. The variation of RF with $G/E_{min}$ for different values of $E_1/E_2$ is plotted in Fig. 5, where G is the shear modulus of rock mass and $E_1$ and $E_2$ are the moduli of deformation of rock mass in horizontal and vertical directions respectively.

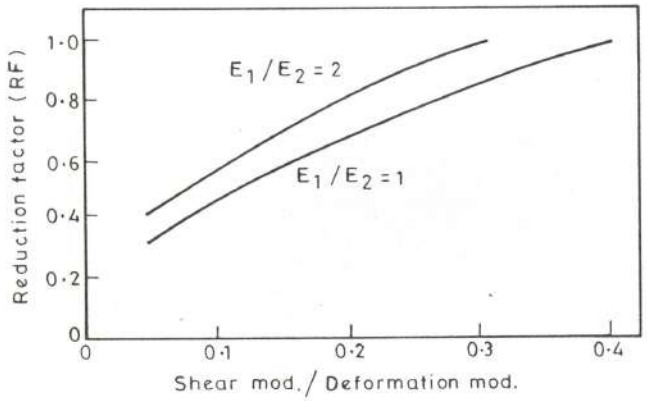


Fig. 5 - Reduction factor for anisotropic rock mass (Kumar and Singh, 1990)

## 7. EXPRESSION FOR SUPPORT PRESSURE IN SQUEEZING GROUND CONDITIOIN AND EFFECT OF TUNNEL SIZE

Expression for short-term support pressure in squeezing ground condition may be obtained by equating the radial tunnel closure (Eqs. 7a, b, c presented in Part-I of this

paper, Viladkar et al., 2008) obtained from ground response and support reaction curves, since these two values are equal at the point of intersection of the two curves. This results in the following expression for the case of a constant volume expansion, e throughout the broken zone (Eq. 7a),

$$p_{if} = \frac{1-[(1+e)-(b_f/a)^2 e - 2(b_f/a)u_b + (u_b/a)^2]^{1/2}}{(s.a/A_s.E_s)+(0.86a^{1.05}/t_b.E_{bf})} \qquad (12a)$$

where $b_f$ is the final radius of the broken zone corresponding to $p_i = p_{if}$ and may be obtained in terms of $p_{if}$ from Eq. 6 of Part I of this paper (Viladkar et al., 2008) with, $0.5\,(\sigma_{re} + \sigma_{\theta e})$ replaced by $p_o$, for hydrostatic in-situ stress field which may be rewritten as follows for $p_i = p_{if}$ and $b = b_f$ :

$$\text{If} \quad P = p_o\,(1 - \sin\phi_p) - c_p \,.\, \cos\phi_p \,,$$

$$\text{then} \quad p_{if} = [P + c_r \cot\phi_r]\,(a/b_f)^{\alpha} - c_r \,.\, \cot\phi_r \pm \gamma.a.[(1-\sin\phi_r)/(1-3\sin\phi_r)]\,[(a/b_f)^{\alpha-1} - 1] \qquad (12b)$$

Nature of Eqs. 12a and 12b is such that the value of $p_{if}$ has to be obtained by an iterative process using Eq. 12a. Derivation of Eq. 12a is presented in Appendix C. Radius of final broken zone, $b_f$ may be deduced from the readings of multiple borehole extensometer within the broke zone (Jethwa, 1981). Observed radial displacements at any time within the elastic zone are relatively independent of time. Data also gives the radius of compaction zone ($\xi$) within the broken zone which is difficult to predict theoretically. Further research is therefore needed to consider highly time-dependent rock mass - tunnel support interaction in the squeezing ground condition. Eq. 12a may be used for evaluation of the effect of tunnel size on short-term support pressure. It may be seen from this equation that short-term support pressure is practically independent of the tunnel size if $A_s/s$ and $t_b$ are increased in direct proportion to the tunnel size.

Like the case of elastic non-squeezing ground condition (Eq. 11b), Eq. 12a may also be generalized to include the effect of anisotropy of rock mass, in the form –

$$p_{if} = \frac{1-[(1+e)-(b_f/a)^2 e - 2(b_f/a)u_b + (u_b/a)^2]^{1/2} - (u_{ao}/a)}{(s.a/A_s.E_s)+(0.86a^{1.05}/t_b.E_{bf})} \qquad (12c)$$

where, $u_b$ can be obtained from Eq. 7d of Part I of this paper (Viladkar et al., 2008) by replacing $E_d$ with $RE.E_{min}$ as -

$$u_b = \frac{(1+\nu)(p_o - p_b)b_f}{RF.E_{min}} \qquad (12d)$$

where $p_b$ is radial stress at elastic- plastic boundary ($r = b_f$) as per Eq. 12b of Part I of this paper (Viladkar et al., 2008).

## 8. EMPIRICAL CORRELATION FOR STAND-UP TIME

It is important to know the time period for which a tunnel section can be left unsupported. Knowledge of this time period helps in determining the time by which installation of the supports may be delayed and the initial displacement, $u_{ao}$, which may be permitted. Bieniawski (1989) related the stand-up time with RMR and roof span and plotted the results in the form of a chart (Figs. 6 a, b). The chart does not consider the effect of the excavation shape and gives the same value of stand-up time for a given opening size and RMR, regardless of the shape of the opening. However, excavation shape is likely to influence the stand-up time (Lauffer, 1958).

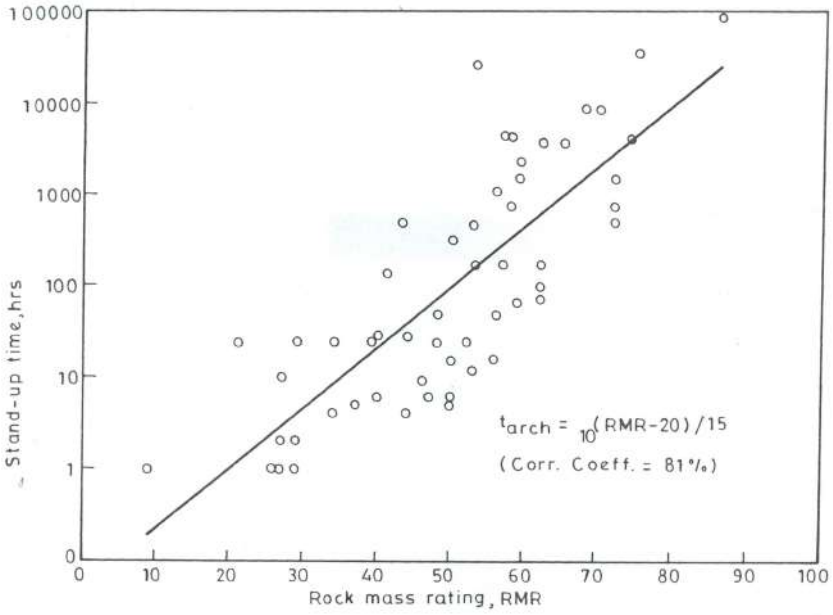


Fig. 6a - Correlation between stand – up time and RMR for underground openings with arch roof

### 8.1 Effect of RMR on Stand-up Time

To overcome the above problem, Bieniawski's (1989) data has been re-analyzed to arrive at an empirical correlation for stand-up time. Mining and the tunnelling (including caverns) cases were separated for this purpose as these normally have different excavation shapes i.e. flat roof and arch roof respectively. An analysis of Bieniawski's data has revealed that RMR has a dominating influence on the stand-up time. Figures 6a and 6b display his data plotted as RMR versus stand-up time for arch and flat roofs respectively. The following correlations have been obtained from the regression analysis for underground openings with arch and flat roofs (i.e. tunneling and mining case respectively):

$$t_{arch} = 10^{(RMR-20)/15} \quad \text{hrs} \qquad (13a)$$

with a correlation coefficient = 81% and

$$t_{flat} = 10^{(RMR - 23)/14} \quad \text{hrs} \qquad (13b)$$

with a correlation coefficient = 96% where, $t_{arch}$ and $t_{flat}$ are the stand-up times for opening with arch roof and flat roof respectively.

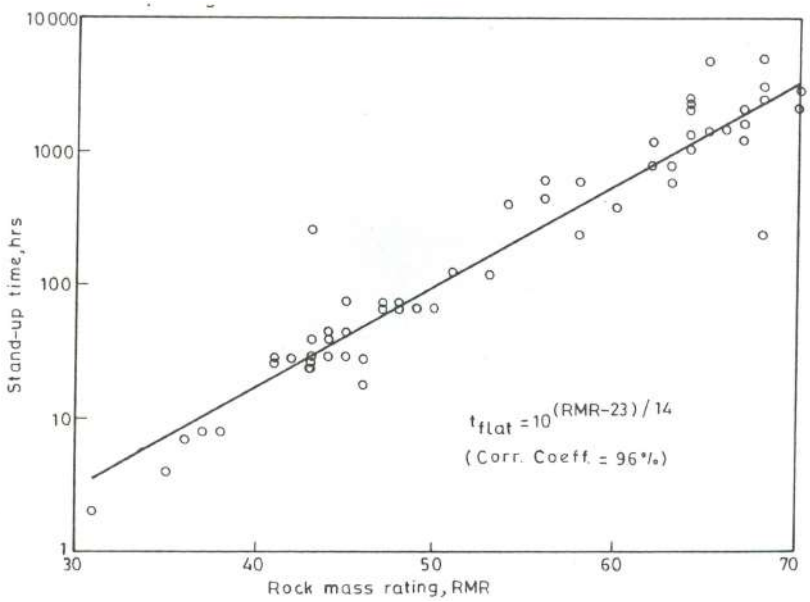


Fig. 6b - Correlation between stand – up time and RMR for underground openings with flat roof

### 8.2 Effect of Opening Size and Overburden Height on Stand-Up Time

To study the effect of opening size, correction factors $f_{arch}$ and $f_{flat}$ (for arch and flat roofs respectively) were built in Eqs. 13a and 13b and the correction factors are therefore defined as:

$$f_{arch} = \frac{t_{arch}^{obsd}}{10^{(RMR-20)/15}} \qquad (14a)$$

and

$$f_{flat} = \frac{t_{arch}^{obsd}}{10^{(RMR-23)/14}} \qquad (14b)$$

where $t_{arch}^{obsd}$ and $t_{flat}^{obsd}$ are the observed stand-up times for openings with arch roof and flat roof respectively. Regression analysis gave the following correlations for correction factors calculated from these equations:

$$f_{arch} = B^{-(0.004\,H - 0.21)} \qquad (15a)$$

and

$$f_{flat} = B^{-(0.014\,H - 0.24)} \qquad (15b)$$

Applying these correction factors, correlations for the stand-up times (Eqs. 13 a, b) may be expressed as:

$$t_{arch} = 10^{(RMR - 20)/15} . B^{-(0.004\,H - 021)} \quad \text{hrs} \qquad (16a)$$

and

$$t_{flat} = 10^{(RMR - 23)/14} . B^{-(0.014 H - 0.24)} \quad \text{hrs} \qquad (16b)$$

where B and H represent the width of the opening and overburden in meters, respectively. It may be seen from these equations that stand-up time decreases with increase in opening size, B. Further, the size effect depends upon the height of overburden, H. The size effect is more pronounced in deeper openings than those located at shallow depths.

### 8.3 Correction Factors for obtaining $t_{arch}$ from $t_{flat}$ and Effect of Opening Shape

Equations 16a and 16b further indicate that opening size influences the stand-up time more in case of arch roof openings than in case of flat roof openings. This, however, does not appear to be correct. This anomaly is due to the fact that stand-up time depends upon the active span of the opening and not on its total span as considered in these equations. The active span (unsupported span) is defined as the distance of the last support from the tunnel face or the tunnel span, whichever is minimum. The data reported and used in Figs. 6 a and 6b by Bieniawski (1989) shows the total span of the opening and not its active span. It is therefore futile to seek a correlation for stand-up time including the effect of opening size from this data. Equations 14a and 14b therefore may not be used directly for estimating the stand-up time. Further analysis has revealed that the correlation coefficients of Eqs. 16a and 16b are only marginally better than those of Eqs. 13a and 13b. In view of this, Eqs. 13a and 13b may be used to determine the ratio of stand-up time of the arch roof openings to that of the flat roof openings. This is given as:

$$f_t = 10^{-(RMR - 65)/100} \geq 1 \qquad (17)$$

where, $f_t = t_{arch} / t_{flat}$

$f_t$ may be used as the correction factor for obtaining $t_{arch}$ from the following equation:

$$t_{arch} = f_t . t_{flat} \qquad (18)$$

For using Eq. 18, $t_{flat}$ may be obtained from Fig. 6b (Bieniawski, 1989) and $f_t$ may be picked up from Fig. 7. Equation 17 shows the influence of the shape of an underground opening on the stand-up time. It may be seen from Fig. 7 that this effect is more pronounced in openings driven through relatively poor rock masses (i.e. with low RMR values), goes on reducing with the improvement in the rock mass quality and finally becomes non-existent (=1) for RMR value of 65 and above.

## 9. CONCLUSIONS

Work presented in this paper is based on field studies carried out at 63 different sections in tunnels of various projects in the Lower Himalaya and peninsular India. The field studies involved instrumentation and monitoring of data related to – a) tunnel convergence / closure, b) deep seated deformations in rock mass, c) contact pressures between rock mass and steel sets and iv) loads in steel ribs apart from other data related

to geometry and rock mass classification. This field data was analyzed with the aim of proposing a practical approach for prediction of ground response and support reaction curves for both self supporting/non-squeezing and squeezing ground conditions in order to perform a complete rock mass-tunnel support interaction analysis. Based on the analysis of the field data collected at tunnel project sites in India and the field data available in the literature, empirical correlations have been derived and presented in this Part II of the paper for –

(i) Stiffness of the backfill between steel rib and rock (Eq. 4).
(ii) Stiffness of the support system with different types of backfills for determination of the support reaction curve (Eqs. 5 a -c).
(iii) Additional pressure on the support system due to charging of the concrete- water conductor system and post construction saturation of argillaceous rock masses (Eq. 8)

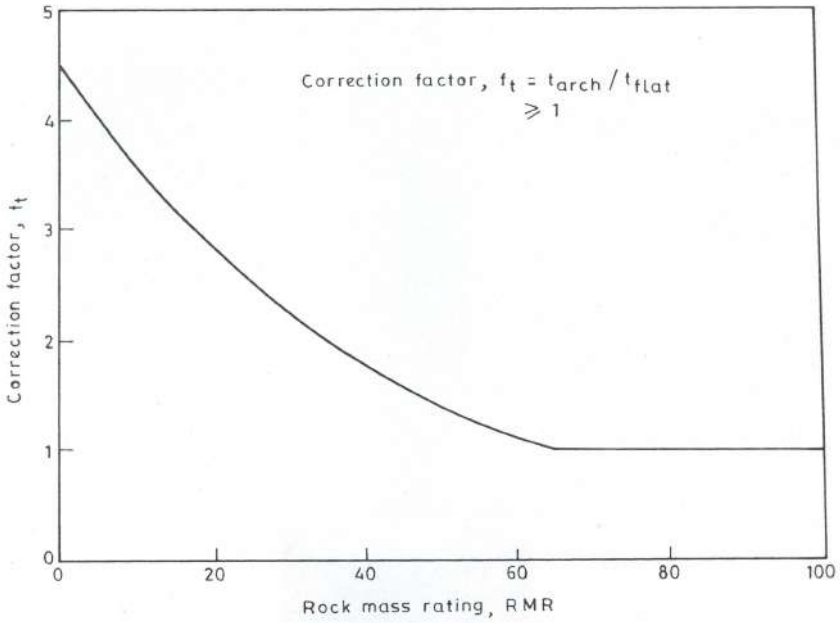


Fig. 7 - Variation of correction factor (Ratio of stand – up time of arch and flat openings) with RMR

(iv) Short term support pressures for both non-squeezing ground condition (Eqs. 11 a and 11b) and squeezing ground condition (Eqs. 12 b and 12c) and
(v) Prediction of stand-up time for underground openings with flat and arch roof shapes (Eqs. 17 and 18). Figure 7 shows that the stand up time is much higher for arch roof than for flat roof in mines.

**References**

Bieniawski, Z.T. (1989). Engineering rock mass classification, John Wiley and Sons, p. 251.

Daemen, J.J.K. (1975). Tunnel support loading caused by rock failure, Technical Report MRD-3-75, Missouri River Division, U.S. Corps. of Engineers, Omaha, Neb.

Hoek, E. and Brown, E.T. (1980). Empirical strength criterion for rock masses, Journal of the Geotechnical Engineering Division, ASCE, Vol. 106, No. GT9, pp 1013-1035.

Indraratna, B. and Kaiser, P.K. (1990). Design for grouted rock bolts based on the convergence control method, International Journal of Rock Mechanics and Mining Sciences, Vol. 27, No. 4, pp 269-281.

Jethwa, J.L. (1981). Evaluation of rock pressures in tunnels through squeezing ground in lower Himalayas, Ph.D. Thesis, Deptt. of Civil Engg., University of Roorkee, Roorkee, India, p. 272.

Kumar, P. and Singh, Bhawani (1990). Design of reinforced concrete lining in pressure tunnels considering thermal effects and jointed rock mass, Tunnelling and Underground Space Technology, Vol. 5, No. ½, pp 91-101.

Ladanyi, B. (1974). Use of the long-term strength concept in the determination of ground pressure on tunnel linings, Advances in Rock Mechanics, Proc. 3rd Congress of the International Society for Rock Mechanics, Vol. 2, Part B, National Academy of Sciences, Washington, D.C., pp 1150-1156.

Lauffer, H. (1958). Gebirgsklassifizierung fur den stollenbau, Geologie und Bauwesen, Vol. 24, No. 1, pp. 46 – 51.

Lombardi, G. (1970). Influence of rock characteristics on the stability of rock cavities, Tunnels and Tunnelling, Vol. 2, No. 1, Jan.-Feb., London, England, pp. 19-22, Vol. 2, No. 2, Mar.-Apr., pp 104-109.

Lombardi, G. (1973). Dimensioning of tunnel linings with regard to constructional procedure, Tunnels and Tunnelling, Vol. 5, pp 340 – 351.

Mehrotra, V.K. (1992). Estimation of engineering parameters of rock mass, Ph.D. Thesis, Department of Civil Engineering, IIT Roorkee, India, p. 267.

Mitri, H.S. and Hassan, F.P. (1990). Structural characteristics of coal mines steel arch supports, International Journals of Rock Mechanics and Mining Sciences, Vol. 27, No. 2, pp. 121-127.

Singh, Bhawani, (1973). Continuum characterization of jointed rock mass, International Journal of Rock Mechanics and Mining Sciences, Vol. 10, pp 311-349.

Singh, Bhawani, Jethwa, J.L., Dube, A.K. and Singh, B. (1992). Correlation between observed support pressure and rock mass quality, Tunneling and Underground Space Technology, Vol. 7, No. 1, pp 59-74.

Stille, H., Holmberg, M. and Nord, G. (1989). Support of weak rock with grouted bolts and shotcrete, International Journal of Rock Mechanics and Mining Sciences, Vol. 26, No. 1, pp. 99-113.

Timoshenko, S.P. and Gere, J.M. (1961). Theory of elastic stability, 2nd Edition, McGraw Hill Book Co.

Verman, Manoj (1993), Rock mass – tunnel support interaction analysis, Ph.D. Thesis, Department of Civil Engineering, IIT Roorkee, India, p. 267.

Viladkar, M. N., Verman, M., Singh, B. and Jethwa, J. L. (2008). Rock mass – tunnel support interaction analysis: Part I - Ground response curves (in this issue of Journal).

## APPENDIX – A

### ADDITIONAL SUPPORT PRESSURE DUE TO CHARGING OF WATER CONDUCTOR SYSTEM

From Fig. 5 (in Part I of this paper, Viladkar et al. 2008) for non-squeezing ground condition,

$$u_a = (1+\nu)(p_o - p_i) / E_d \quad (A.1)$$

Rewritten Eq. A.1 for dry and saturated rock mass conditions (i.e., before and after charging of the water conductor system) and equating the right hand sides of the resulting equations (tunnel closure is the same for both the conditions as shown in Fig. 4),

$$(1+\nu)(p_o - p_{i\,dry}) / E_{dry} = (1+\nu)(p_o - p_{i\,sat}) / E_{sat} \quad (A.2)$$

where, $p_{isat}$ = support pressure in saturated condition.

From Eq. A.2, on multiplying both sides by $E_{sat}$,

$$p_{isat} = p_o [(1-E_{sat} / E_{dry})] + p_{i\,dry} (E_{sat} / E_{dry})$$

or

$$\Delta p_{isat} = p_o [(1- (E_{sat} / E_{dry})] - p_{i\,dry} [(1- (E_{sat} / E_{dry})] \quad (A.3)$$

where,

$$\Delta p_{isat} = (p_{i\,sat} - p_{i\,dry})$$

Equation A.3 may be written as,

$$\Delta p_{isat} = [(1-E_{sat} / E_{dry})] (p_o - p_{i\,dry}) \quad (A.4)$$

which is the same as Eq. 8.

## APPENDIX – B

### EXPRESSION FOR SUPPORT PRESSURE IN NON-SQUEEZING GROUND CONDITION

From Eq. 5 (in Part I of this paper, Viladkar et al., 2008) for ground reaction curve in non-squeezing ground condition,

$$u_{ag} = (1+\nu)\,(p_o - p_{ig}) / E \qquad \text{(B.1)}$$

From Eq. 1 (in Part II) for support reaction curve,

$$u_{as} = (u_{ao} / a) + (p_{is} / k) \qquad \text{(B.2)}$$

where the subscripts 'g' and 's' refer to the ground response and the support reaction curves respectively.

At the point of intersection of the two curves, $u_{ag} = u_{as}$. At this point, therefore, the right hand sides of Eqs. B.1 and B.2 may be equated. This, together with the substitution of both $p_{ig}$ and $p_{is}$ with $p_{if}$ for the point of intersection, results in the following equation :

$$(1+\nu)\,(p_o - p_{if})\,/\,E_d = (u_{ao} / a) + (p_{if} / k) \qquad \text{(B.3)}$$

or,

$$p_{if}\,[(1+\nu) / E_d + (1 / k)] = [(1+\nu)\,p_o / E_d - (u_{ao} / a)]$$

or,

$$p_{if} = \frac{[(1+\nu)p_o / E_d - (u_{ao} / a)}{[(1+\nu) / E_d + (1/k)} \qquad \text{(B.4)}$$

Substituting the expressions for 1/ k in Eq. B.4 from Eqs. 2, 3 and 4 gives,

$$p_{if} = \frac{[(1+\nu)p_o / E_d - (u_{ao} / a)}{[(1+\nu) / E_d] + (s.a / E_s.A_s) + (0.86a^{1.05} / t_b.E_{bf})} \qquad \text{(B.5)}$$

which is the same as Eq. 11a.

## APPENDIX-C

## EXPRESSION FOR SUPPORT PRESSURE IN SQUEEZING GROUND CONDITION

From Eq. 7a (Viladkar et al., 2008) for ground response curve in squeezing ground condition,

$$u_{ag}/a = 1 - [(1+ e) - (b / a)^2 e - 2 (b / a) u_b + (u_b / a)^2]^{1/2} \quad (C.1)$$

From Eq. 1 in Part II of this paper for support reaction curve,

$$u_{as} / a = (u_{ao} / a) + (p_{is} / k) \quad (C.2)$$

where the subscripts 'g' and 's' refer to ground response and support reaction curves respectively.

At the point of intersection of the two curves, $u_{ag} = u_{as}$. At this point, therefore, right hand sides of Eqs. C.1 and C.2 may be equated. This, together with the substitution of b with $b_f$ and $p_{is}$ with $p_{if}$ for the point of intersection, results in the following equation :

$$1- [(1+ e) - ( b_f / a)^2 e - 2 ( b_f / a) u_b + (u_b / a)^2]^{1/2} = (u_{ao} / a) + (p_{if} / k) \quad (C.3)$$

or,

$$p_{if} = \frac{1-[(1+e)-(b_f/a)^2 e - 2(b_f/a)u_b + (u_b/a)^2]^{1/2} - (u_{ao}/a)]}{1/k} \quad (C.4)$$

Substituting expressions for 1/k in Eq. C.4 from Eqs. 2, 3 and 4 gives,

$$p_{if} = \frac{1-[(1+e)-(b_f/a)^2 e - 2(b_f/a)u_b + (u_b/a)^2]^{1/2} - (u_{ao}/a)]}{(S.a / A_s.E_s) + (0.86a^{1.05} / t_b.E_{bf})} \quad (C.5)$$

which is the same as Eq. 12a.